Journal of Materials and Environmental Science ISSN: 2028-2508

e-ISSN: 2737-890X CODEN: JMESCN Copyright © 2025, University of Mohammed Premier Oujda Morocco J. Mater. Environ. Sci., 2025, Volume 10, Issue 10, Page 1924-1939

http://www.jmaterenvironsci.com



Removal of ofloxacin from the aqueous medium by adsorption on activated carbon from coconut shells

ODI Assemien Prisca Elodie^{1*}, SORO Donafologo Baba^{1**}, ACHO Yapi Fulgence¹, N'ZUE Yao Jean Vianney¹, N'GUETTIA Kossonou Roland¹, YAYA Coulibaly², MEITE Ladji¹, ABOUA Kouassi Narcisse¹, TRAORE Karim Sory¹

¹Laboratory of Environmental Sciences, UFR of Environmental Sciences and Management, Nangui Abrogoua University, Abidjan 02, Ivory Coast,

²UFR-Agriculture, Fisheries Resources and Agro-industry, University of San-Pedro, San-Pedro 01, Ivory Coast

* Corresponding author, Email address: <u>assemienelo@gmail.com</u>
** Corresponding author, Email address: <u>baba_soro@yahoo.fr</u>

Received 23 Jul 2025, **Revised** 02 Oct 2025, **Accepted** 04 Oct 2025

Citation: Odi A.P.E., Soro D.B., Acho Y.F., N'zue Y.J.V., N'guettia K.R., Yaya C., Meite L., Aboua K.N., Traore K.S. (2025) Removal of ofloxacin from the aqueous medium by adsorption on activated carbon from coconut shells, J. Mater. Environ. Sci., 16(10), 1924-1939 **Abstract:** The objective is to test the effectiveness of an activated carbon prepared from coconut shells for the elimination of ofloxacin in solution. The raw material has been crushed and the diameters chosen are between 1 and 2 mm. This shredded material was activated with 50 % orthophosphoric acid at a ratio of 0.5 and then calcined at 500 °C for 2 hours. Chemical characterization tests were carried out and concern the specific surface area, iodine value, surface functions and pHpzc. The specific surface area of the coal was determined by the BET method. The results reveal that the prepared activated carbon has an iodine value of 675.64 mg/g and a specific surface area of 1195 m²/g, which is essentially microporous. It exhibits an acidic character due to its carboxylic and phenolic functions, with a pHpzc value of 2.9. The influence of specific parameters such as pH, carbon dose, and initial concentration of the adsorbate showed the effectiveness of the adsorbent with more than 99% removal of ofloxacin. The study shows that the prepared activated carbon is a promising adsorbent.

Keywords: Adsorption; Ofloxacin; activated carbon; coconut shells

1. Introduction

With the continuous development of science and technology as well as the process of industrialization, various types of drugs, dyes, and heavy metals are widely used for the treatment and prevention of diseases (Klein *et al.*, 2018; Allen and Nilsson, 2021; Aaddouz *et al.*, 2023; Kumar *et al.*, 2025). The rapid pace of industrialization has contributed to environmental pollution, particularly in water, a vital source of life and energy. These drugs are released by households, health centres, or farms after use, from formulation sites, garbage dumps, or accidental spills, and are increasingly found in the aquatic environment (Aydin and Talinli, 2013). Since the 1980s, numerous studies have been conducted on the presence of drug residues in wastewater. This research showed the presence of traces of several organic and inorganic compounds. For example, the presence of residues from drug products in wastewater for several years has been a significant area of concern (Thomas, 2015). Among these products, a considerable amount of antibiotics is used and regularly released into the atmosphere by

pharmaceutical industries, hospitals, domestic wastewater, excretions of living beings, etc (El-Ghenymy, 2013; Salem *et al.*, 2015; Abuduxike and Aljunid, 2012). Ofloxacin is one of the most widely used antibiotics in poultry and aquaculture worldwide, and its massive use poses a huge threat to the environment (Nguyen, 2021). This is because this molecule inhibits the physiological processes of algae's natural photochemical and antioxidant systems, reducing algal cell growth, chlorophyll content, and photosynthesis rate. More importantly, increased ofloxacin residues in the environment may lead to increased drug resistance (Lahouidak *et al.*, 2019; Wang *et al.*, 2022). In addition, ofloxacin may cause acute toxicity to aquatic organisms at concentrations of the order of mg/L and chronic toxicity at concentrations of the order of μg/L (Chaturvedi *et al.*, 2021; Wang *et al.*, 2021). It is therefore necessary to effectively remove it from the aqueous medium.

Several methods have been used, such as biological methods (Sbardella *et al.*, 2018) Sonochemical (Hapeshi *et al.*, 2010), adsorption on carbon-composites (Chunmiao *et al.*, 2018; Akartasse *et al.*, 2022), and ozonation (Madehi and Tay, 2015). However, low efficiency, high cost, and the generation of toxic by-products limit the large-scale application of these methods. On the other hand, adsorption has proven to be an effective treatment technique in water treatment. One of the most commonly used adsorbents, which is commercial activated carbon, is proving to be very expensive. As an alternative, especially for underdeveloped countries like ours, research is directed towards materials such as abundant agricultural waste that can be transformed into activated carbon, which is also effective for water treatment. It is in this context that this study is carried out, to test the effectiveness of an activated carbon prepared from coconut shells for the elimination of ofloxacin in solution.

2. Materials and methods

2.1 Preparation of activated carbon

The coconut shells were collected in the town of Jacqueville, located in the south of Ivory Coast, 60 km from Abidjan, from the vendors. They were air-dried in the laboratory before being crushed and sieved to extract the fraction of particles of homogeneous sizes between 1 and 2 mm. The fraction thus selected was washed several times with tap water and then distilled water to remove impurities, then dried at 110 °C for 24 hours in a Memmert oven. After drying, the samples were impregnated for 24 h in a 50 % orthophosphoric acid solution and then calcined at 500 °C for 2 h in a branded muffle furnace Nabertherm with a heating speed of 10 °C /min. After carbonization, the activated carbon obtained with a CAC rating is cooled and then washed several times with distilled water until the pH of the washing water reaches a neutral level. It is dried in the oven at 110 °C for 24 hours.

2.2 Solvents and Reagents

The ofloxacin (OFL) used with 98% purity comes from the company Sigma Aldrich. Its chemical structure is illustrated in **Figure 1**. The acetonitrile and formic acid used for chromatographic analyses are of analytical or superior quality and are marketed by the companies Prolabo and Carlo Ebra, respectively.

Figure 1. Chemical structure of OFL

2.3 Characterization of activated carbon

2.3.1 Fourier Transform Infrared Spectrometry (FTIR)

Infrared analysis was performed using a Fourier transform spectrophotometer (FTIR) over a wavelength range of 400–4000 cm⁻¹ with a resolution of 4 cm⁻¹. A small amount of the adsorbent is crushed with pure, dry potassium bromide (KBr). The mixture obtained is compressed under the effect of high pressure and in a vacuum; to form a plate of parallel faces or transparent pellets, the latter is placed in the path of the light beam. The analysis has been done.

2.3.2 Surface Functions

The total acidity and basicity of the samples are determined by titration with NaOH and HCl using the Boehm method. A mass of activated carbon of 0.4 g shall be mixed with 20 mL of one of the following acidic or basic compounds with a concentration of 0.1M: NaHCO₃, Na₂CO₃, NaOH and HCl. The whole thing was agitated for 24 hours. After agitation, 10 mL of filtrate is collected and titrated with 0.1M NaOH or 0.1M HCl as appropriate. The equivalents were calculated using the equation below:

$$N_{\text{éq}} = N_0 V_0 - N_f V_0$$
 Eqn. 1

Neq: the number of gram equivalents that reacted; N_0V_0 : the number of gram equivalents before the reaction; N_fV_0 : Number of Gram Equivalents After Reaction

2.3.3 point of zero charge (pHpzc)

According to the protocol proposed by Rivera-Utrilla *et al.*, 2013, 0.15 g of CAC was introduced into 50 mL of a NaCl solution with a concentration of 0.01 M and a pH between 2 and 12. The pH was adjusted using an HCl solution and a NaOH solution with a concentration of 0.01 M. The suspensions were then stirred for 24 hours at room temperature, after which the final pH (pHf) was measured. Δ pH (pHf – pHi) is then plotted as a function of the initial pH of the solution. The intersection of this curve with the x-axis gives the pH value to the point of zero charge.

2.3.4 Iodine Value

The iodine value is determined according to the standard method ASTM-D-4607 (Tra *et al.*, 2024). A mass of 0.5g of CAC is introduced into a beaker and to this is added 20 ml of the iodine solution of concentration 0.05N. The whole thing is stirred for 5 minutes and then filtered. After filtration, 10 mL of the filtrate is titrated with sodium thiosulphate with a concentration of 0.05N until the solution is completely discoloured. The iodine value expressed in mg/g is given by the relationship below:

$$I_{2}(mg/g) = \frac{\left[C_{0} \frac{C_{n} \times V_{n}}{2VI_{2}}\right] \times MI_{2} \times V_{abs}}{m}$$
 Eqn. 2

- C_0 and C_n represent respectively the initial concentration (mol.L⁻¹) of iodine and the concentration of sodium thiosulphate solution (mol.L⁻¹);
- V_n , VI_2 and V_{abs} , are the respective volumes of the thiosulphate solution at equivalence, the volume of the dosed iodine solution (10 mL) and the absorbed volume;
- MI₂ is the molecular weight of iodine (mol.L⁻¹) and m is the mass of activated carbon (g).

2.3.5 Porosity and Specific Surface Area

2.3.5.1 Porosity

The size distribution of mesopores and macropores is calculated according to the Barret, Joyner and Helenda method (BJH method). The BJH method is used to determine the volumes and surfaces accumulated by pores with widths between 17 Å and 3000 Å (mesopores and macropores) during N adsorption₂. The presence of micropores is observed from the adsorption isotherms and the specific surface.

2.3.5.2 Specific surface area for the BET

The test is performed on a bed of activated carbon particles at atmospheric pressure. The adsorbed body is nitrogen mixed with helium (carrier gas). The bed of carbon contained in a glass ampoule has previously been degassed at medium temperature (300-350°C) for 4 to 5 h under pressures reduced by 2 mbar. Degassing makes it possible to rid the solid of impurities that would occupy the pores. The BET equation used in practice in its linear form is:

$$\left(\frac{(P/Po)}{Qads(1-P/Po)}\right) = \frac{1}{Qm*C} + \frac{(C-1)}{Qm*C} - \frac{P}{Po}$$
 Eqn. 3

Indeed, the graph obtained by the values of the first member of the BET equation as a function of $p/p\left(\frac{(P/Po)}{Qads\,(1-P/Po)}\right)_0$ allows us to determine the specific surface area with the following relationship:

$$SBET = \sigma N_{AQm}$$
 Eqn. 4

 σ : Surface occupied by a molecule of steam;

 N_A : Avogadro number (6.025.10²³ mol⁻¹);

Qm: the amount of gas needed to coat 1g of adsorbent

2.4 Adsorption Experiments

Adsorption tests ofloxacin on the CAC were carried out in batch mode in a beaker at room temperature (25 °C). Thus, a weighed quantity of CAC is introduced into the beaker containing 500 mL of solution ofloxacin at a known concentration. The whole thing was stirred and samples were taken at regular intervals. The samples were analysed using a high-performance liquid chromatograph (HPLC) from Schambeck SFD GmbH in order to monitor the evolution of the residual concentration of the molecule.

Chromatographic analysis conditions: The mobile phase consisted of formic acid (45 %) and acetonitrile (55 %). The stationary phase was a Pursuit 5 C18 column (250 mm x 4.6 mm, 5 μ m) in isocratic mode. The detection wavelength was 293 nm and the injection volume was 20 μ L.

2.4.1 Effect of a few parameters on adsorption kinetics

2.4.1.1 Influence of Adsorbent Mass

The tests were carried out with different masses of CAC (1; 1.5; 2.5; 3 and 4 g) when contacted with 500 mL of concentration OFL solution $C_0 = 20$ mg.L⁻¹.

2.4.1.2 Influence of pH

The effect of pH was studied by introducing a mass of CAC corresponding to the optimal mass obtained with 500 mL of OFL solution of concentration $C_0 = 20$ mg.L⁻¹. The pH of the solutions

was adjusted to the following values: 2; 4; 6; 7; 9; 11, by adding either a few drops of concentrated HCl or 0.1 M NaOH solutions.

2.4.1.3 Influence of the initial concentration of the solution

The influence of the initial concentration of OFL on the adsorption capacity of CAC was studied for concentrations of 10; 15; 20; 30 and 40 mg/L in the presence of the optimal CAC mass and the optimal pH value.

2.4.2 Adsorption kinetics

Kinetic adsorption modelling of OFL was made according to the following three models (linear form):

✓ Pseudo-first-order kinetic model:

$$Ln(Q_e - Q) = LnQ_e - K_1 t$$
 (Lagergren et al., 1898) Eqn. 5

✓ Kinetic model of the pseudo-second order:

$$\frac{t}{a} = \frac{1}{K_2 O^2} + \frac{t}{O_e}$$
 (Ho *et al.*, 1999) **Eqn. 6**

✓ Kinetic model of intraparticle diffusion:

$$Q = K_n t^{1/2} + C$$
 (Annadurai et al., 2002) Eqn. 7

 K_1 (min⁻¹), K_2 (g/mg.min) and K_p (mg/g.min^{1/2}) are the pseudo-first-order, pseudo-second-order and intraparticle diffusion kinetic constants, respectively.

2.4.3 Adsorption isotherms

The study of the adsorption isotherms makes it possible to determine the adsorption capacity of the adsorbates (OFX) on the adsorbent as well as the type of adsorption mechanism. Two models of adsorption isotherms were used in this study in their linear forms:

• Langmuir:

$$\frac{C_e}{Q_e} = \frac{1}{K_L Q_m} + \frac{C_e}{Q_m}$$
 (Weber *et al.*, 1974) **Eqn. 8**

The separation factor RL is determined by the following relationship:

$$R_L = 1/(1 + K_L C_e)$$

• Freundlich:
$$Ln \ Q_e = Ln \ K_f + \frac{1}{n_f \ Ln \ C_e}$$
 (Calvet *et al.*, 1980) **Eqn. 9**

Q_e: Equilibrium adsorption capacity (mg/g);

C_e: Residual solute concentration at equilibrium (mg/L);

Q_m: Maximum adsorption capacity (mg/g);

K_L: Adsorption equilibrium constant for the solute/adsorbent pair (L/mg);

K_f and n_f: Characteristic constants of the efficiency of an adsorbent with respect to a given solute.

3. Results and discussion

3.1 Characterization of activated carbon

3.1.1 Fourier Transform Infrared Spectrometry (FTIR)

The FTIR is a technique that allows to highlight certain functions such as carboxylic acids, aliphatic chains, aromatics, etc. on the material. Specters IRTF gross CAC (CAC B) and 50% active CAC (CAC 50 %) achieved between 650 and 4,000 cm⁻¹, are presented in the **Figure 2**. The CAC B spectrum has bands at 1702.4; 1586.4; 1196.3; 877.6 and 751.3 cm⁻¹. The band at 1702.4 cm⁻¹ corresponds to elongation vibrations C=O in ketones, aldehydes, lactones or carboxyl groups (Yakut *et al.*, 2016). The band at 1586.4 cm⁻¹ indicates C-C elongation vibrations of the aromatic group. Has 1196.3 cm⁻¹, a characteristic band is observed, vibrations of elongation of the O-H or lactone groups (Blanco *et al.*, 2000). The 877.6 cm⁻¹ can be assigned to the deformations of C-O-H bonds in carboxylic acids. The band observed at 751.3 cm⁻¹ would correspond to alkenic groups, aromatic rings or benzene.

The CAC 50 % spectrum shows the appearance of two new bands and a decrease in intensity or disappearance of those observed on the CAC B spectrum. These results are due to the activation process. Thus, a band at 1691.8 cm-1 is observed, which could be due to the probable formation of new bonds, such as C=O in carbonyl groups (aldehydes or ketones). The same is true for the band at 1550.1 cm⁻¹, which corresponds to the formation of C=C bonds in benzene or aromatic groups (Vunain *et al.*, 2017). These results show the involvement of certain functional groups (hydroxyls, carbonyls, carboxyls) in the adsorption of OFL to the surface of the CAC by electrostatic interaction.

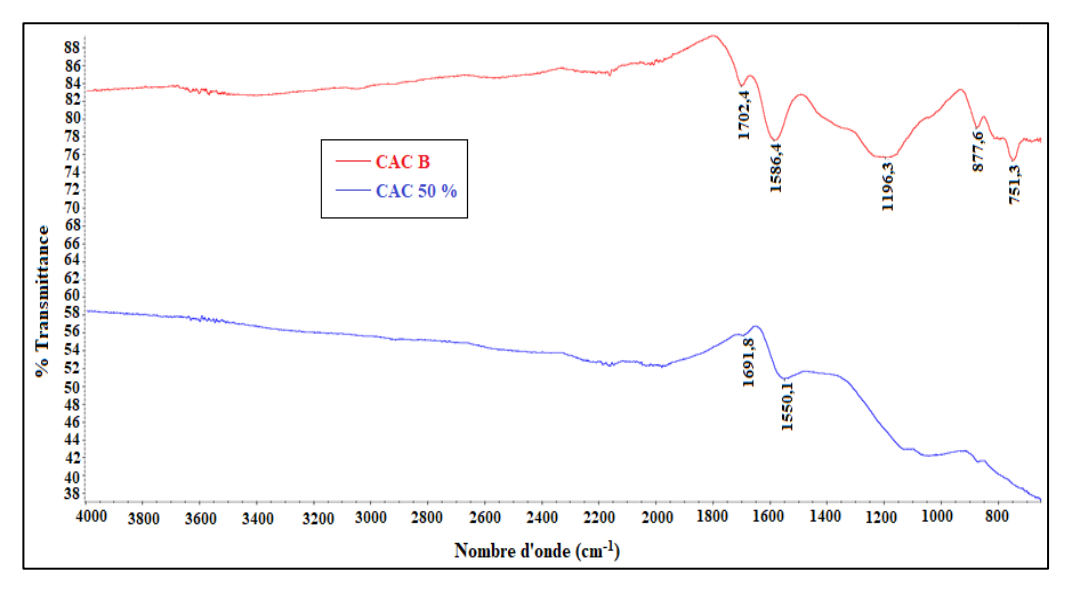


Figure 2. FT-IR spectrum in sample transmission

3.1.2 Surface Function

The surface functions of the developed CAC are presented in the **Table 1**. Given these results, the CAC has a strong acidic character with an average total acidity of 3.225 MEQ/g against an average total basicity of 1.157 meq/g. This acidity is mainly due to the carboxylic (1.817 meq/g) and lactonic (1.0075 meq/g) functions. The presence of both acidic and basic functions predicts the ability of CAC to adsorb both anionic and cationic adsorbates. This can be attributed to the nature of the activating agent, which is a strong oxidant. Thus, surface carbon atoms can be oxidized and lose electrons, becoming positively charged. These charges are responsible for the presence of electrostatic forces of attraction or repulsion between the solute and the adsorbent. Thus, more acidic sites indicate a higher

number of oxygen groups, which allows for high adsorption concerning the chemical nature of the pollutant being treated.

Table 1. Surface	function	concentrations	(meq/g)
------------------	----------	----------------	---------

Function carboxylic	Function phenolic	Function lactonic	Total base	Total acid	Character surface
1.82	0.40	1.01	1.16	3.23	Acid

3.1.3 Point of zero charge (pHpzc)

The point *of* zero charge (pHpzc) is a critical parameter that indicates the acid-base behavior of solids. This is the pH of the solution at which the charge of the positive surface sites equals that of the negative sites, so the surface area of the adsorbent has a value of zero. As shown by **Figure 3**, the value of the pHpzc is 2.9, indicating the acidic character on the surface of the coal. This confirms the acid as already indicated by the results of the Boehm method, which has shown a high proportion of acidic functions (carboxylic and lactonic). When the pH > pHpzc, the surface charge is negative; at pH < pHpzc, it is positive. Similar results are reported in the literature (Sogbochi, 2023).

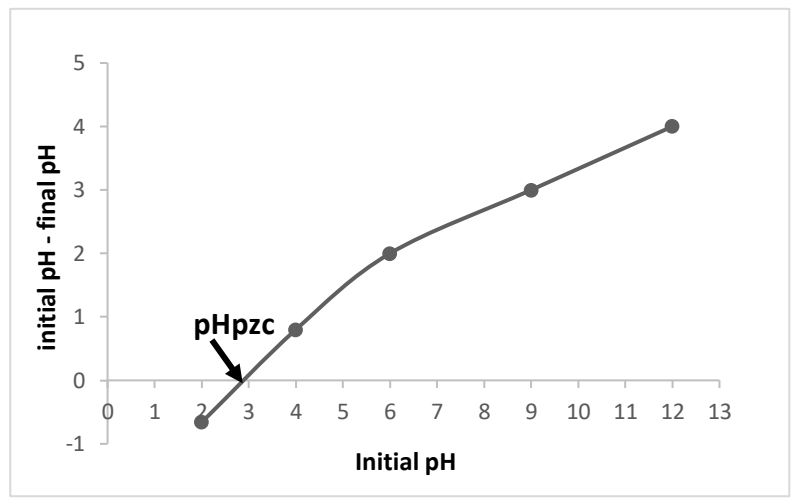


Figure 3. Curve for the determination of pHpzc

3.1.4 Elemental Analysis

The results of the CAC elemental composition are presented in the **Table 2**. It appears that this activated carbon consists mainly of carbon (78.57 %) and oxygen (19.05 %) with a small proportion of hydrogen (2.23 %), nitrogen (0.15 %) and sulphur (0.15 %). Similar results are reported in the literature (Foo *et al.*, 2012; Hidayu *et al.*, 2016).

Table 2. Elemental composition of CAC (% by weight)

Carbon (%)	Oxygen (%)	Hydrogen (%) (%)	Nitrogen (%)	Sulphur (%)	Total
78.57	19.05	2.23	0.15	0.15	100

3.1.5 Specific surface area and porosity

The **Figure 4** presents the CAC N₂/77K adsorption-desorption isotherms. According to the IUPAC classification of adsorption-desorption isotherm curves, the curves obtained would be of type I, reflecting a single-layer adsorption on the surface of the adsorbent. This type of isotherm is common

in the case of activated carbons and is thought to be mainly microporous. The results show that the prepared activated carbon is essentially microporous and mesoporous (**Table 3**). It has a specific surface area of 1195 m²/g and a porous volume of 0,576 cm³/g mostly microporous (0.520 cm³/g). The iodine value obtained (675.64 mg/g) reflects the existence of fairly large micropores on the inner surface of the charcoal. This significant microporosity is linked to the thermal stability of the different components of the coconut shells (lignite, cellulose and hemicellulose) and the activating agent, contributing not only to the creation of new pores, but also to the enlargement of the pores already present in the precursor. This wide distribution of micropores could allow a better diffusion of large molecules within activated carbon.

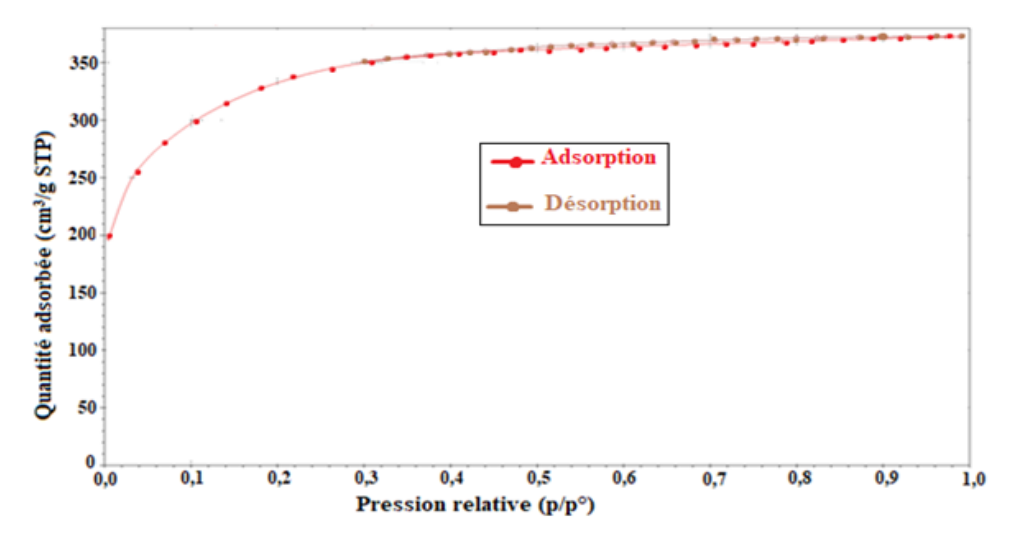


Figure 4. N₂ adsorption and desorption isotherms on the CAC 50 %

Table 3. Specific surface area and porous properties of coal

Specific surface area (m ² /g)	BET	1195
Porous volume (cm³/g)	Point adsorption	0.576
Volume microporeux (cm³/g)	t-Plot	0,520
Mesoporous volume (cm ^{3/} g)	Adsorption BJH BJH desorption	0.056
Iodine Value (mg/g)	Iodometry	675.64

3.2 Adsorption Tests

3.2.1 Effect of Adsorbent Mass

The **Figure 5** illustrates the results obtained. Figure 5A shows an increase in the percentage of adsorption of OFL with increasing CAC mass. Thus, the percentage of adsorption goes from 87.42 % to 99.62 % when the mass of adsorbent increases from 1g to 4g. These results could be explained by the fact that the increase in the mass of coal increases the contact surface and therefore the number of sites available for the fixation of the pollutant, thus favouring the phenomenon of adsorption (Hameed, 2010). On the other hand, a decrease in the amount adsorbed is observed with increasing mass of the adsorbent. Indeed, when the mass of adsorbent increases from 1g to 4g, the adsorption capacity increases from 8.74 mg/g to 2.49 mg/g. This result could be due to the non-saturation of the adsorption sites on the CAC (Patil and Shrivastava, 2010).

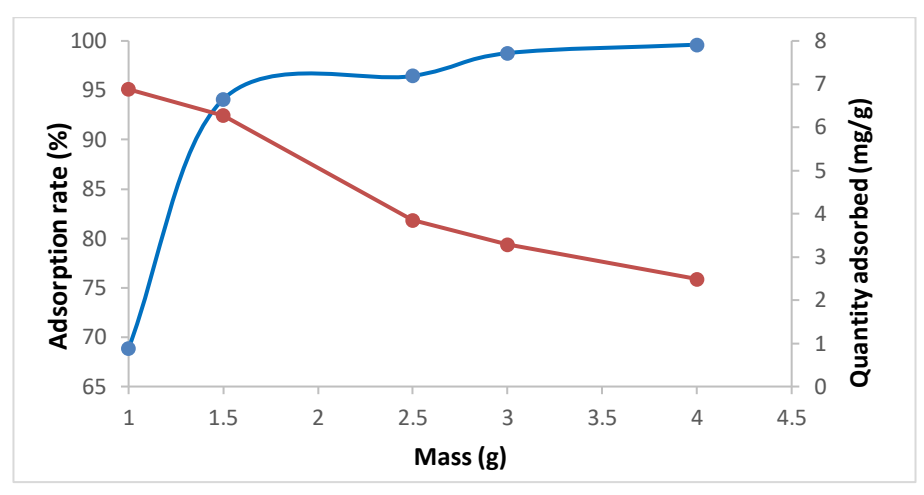


Figure 5. Effect of the coal mass on the adsorption of OFL, Co = 20 mg/L; V = 500 mL; pH = 6

3.2.2 Effect of Solution pH

The pH of the solution is an important factor that affects adsorption and can change the surface load of the adsorbent and OFL species. The adsorption of OFL on the CAC at different pH of the solution is shown on the **Figure 6**. The results showed that the adsorption of this compound is pH-dependent. OFL removal is improved from pH 2 to pH 6. From pH 6, there is a clear decrease in adsorption up to pH 9 and a sharp drop for pH above 9. These results could be attributed to the molecular structural characteristics of OFL and the pHpzc of CAC. Indeed, OFL is an amphoteric molecule with ionizable functional groups. It has two values of pKa (pKa₁ = 5.45 and pKa₂ = 6.2) and can therefore exist in three forms in aqueous solution (Bhatia *et al.*, 2016). It is mainly cationic (OFL⁺) at pH < 6.1 and the anionic form (OFL⁻) is the dominant species at pH > 8.28 (Zhu *et al.*, 2019).

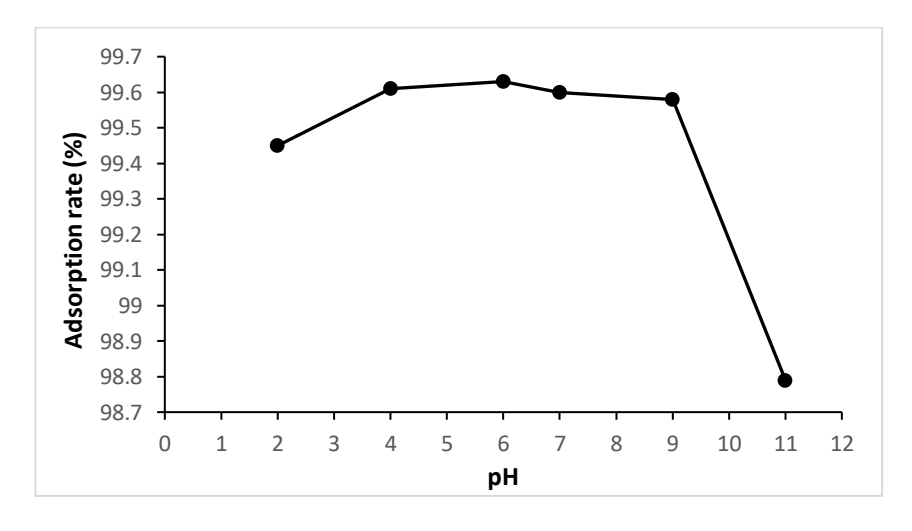


Figure 6. Effect of the pH of the solution on the adsorption of OFL, m = 4 g; V = 500 mL et Co = 20 mg/L

In the pH range 6.1 to 8.28, part of the molecule exists as a zwitterion (OFL \pm) and the rest as a neutral molecule (OFL 0). The pHpzc of CAC determined is 2.9. Thus, the surface of CAC is positively charged when the pH of the solution < 2.9 and negatively charged for the pH > 2.9. Therefore, at pH 6, high ionic interactions occur between the cationic OFL and the CAC surface resulting in high OFL removal. At pH 7, where zwitterion is the dominant species of OFL in solution, a cationic state can still be considered a major contributor to adsorption, from which an appreciable amount of OFL has been

removed from the solution. Above pH 9, the dominant species of OFL is the anionic state providing adsorbent/adsorbate repulsions and consequently, a significant decrease in removal efficiency (Maheshwari *et al.*, 2013). Other authors have reached similar results (Hassan *et al.*, 2014; Lubna *et al.*, 2021).

3.2.3 Effect of the initial concentration

The results of the adsorption tests are shown in Figure 6. This figure shows that an increase in the initial concentration leads to an increase in the removal rate of OFX. This result could be attributed to an increase in the driving force offered by the concentration gradient at high concentrations of OFL (Inbaraj *et al.*, 2006; Hameed *et al.*, 2007). Zabihi *et al.* (2010) and Pandey *et al.* (2010) concluded that increasing the initial concentration of OFL results in a higher probability of collision between the adsorbat molecules and the adsorbent active sites, higher occupancy of the active sites and thus a higher adsorption capacity.

However, beyond the concentration of 20 mg/L, the adsorption rate decreases, indicating the progressive saturation of the charcoal and which would be due to the presence of OFL molecules in excess of the active sites of the adsorbent (Tan *et al.*, 2009). Thus, the highest removal yield of OFL obtained for the initial concentration of 20 mg/L was 99.31 % after 360 min of contact time.

With regard to the quantities adsorbed, it can be observed that an increase in the initial concentration of OFL leads to an increase in the adsorption capacity. Indeed, when the initial concentration of the pollutant increases from 10 to 40 mg/L, the adsorption capacity increases from 1.24 to 4.97 mg/g. The trend line of the adsorbed amount of OFL is linear. According to Dbik *et al.* (2014) who obtained similar results, linearity shows that the number of free sites remains constant during adsorption, meaning that sites are created during this process.

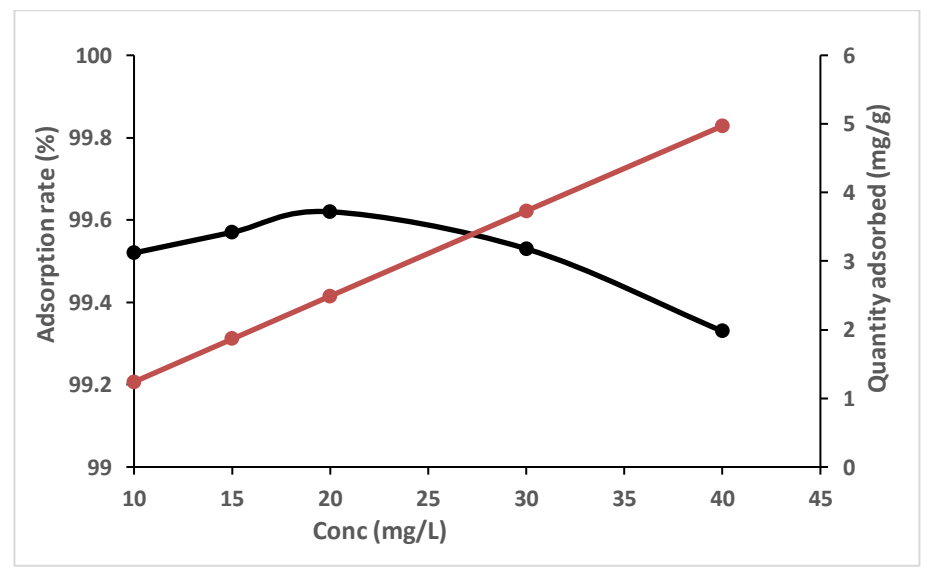


Figure 7. Effect of the initial concentration on the adsorption of OFL, m = 4 g; V = 500 mL; pH = 6

3.3 Modelling of adsorption kinetics

The modelling of the experimental results of the adsorption kinetics of OFL on activated carbon by three models, namely pseudo-first-order, pseudo-second-order and intraparticle diffusion, is presented in the **Figure 8**. The **Table 4** Shows the parameters of these templates.

Table 4. Constants of kinetic models

Co (mg/L)		10	15	20	30	40
Qe (mg/g) exp		1.24	1.87	2.49	3.73	4.97
Pseudo-first	Qe (mg/g) cal	0.85	1.89	4.33	7.19	50.38
Order	$\mathbf{K}_{1}(\mathbf{min}^{-1})$	-0.000072	-0.00009	-0.000034	-0.00004	-0.00089
Oruci	\mathbb{R}^2	0.91	0.89	0.95	0.84	0.87
Pseudo-second	Qe (mg/g) cal	2.38	1.90	1.28	3.44	1.23
Order	$K_2 (\text{mg.g}^{-1}\text{min}^{-1})$	0.09	0.06	0.08	0.03	0.82
01401	\mathbb{R}^2	0.99	0.99	0.99	0.99	0.99
	Qe (mg/g) cal	1.50	2.06	2.79	4.08	4.92
Intraparticle diffusion	$K_p \; (mg/g.min^{1/2})$	0.0619	0.1003	0.1096	0.1854	0.2394
	\mathbb{R}^2	0.76	0.84	0.88	0.98	0.94

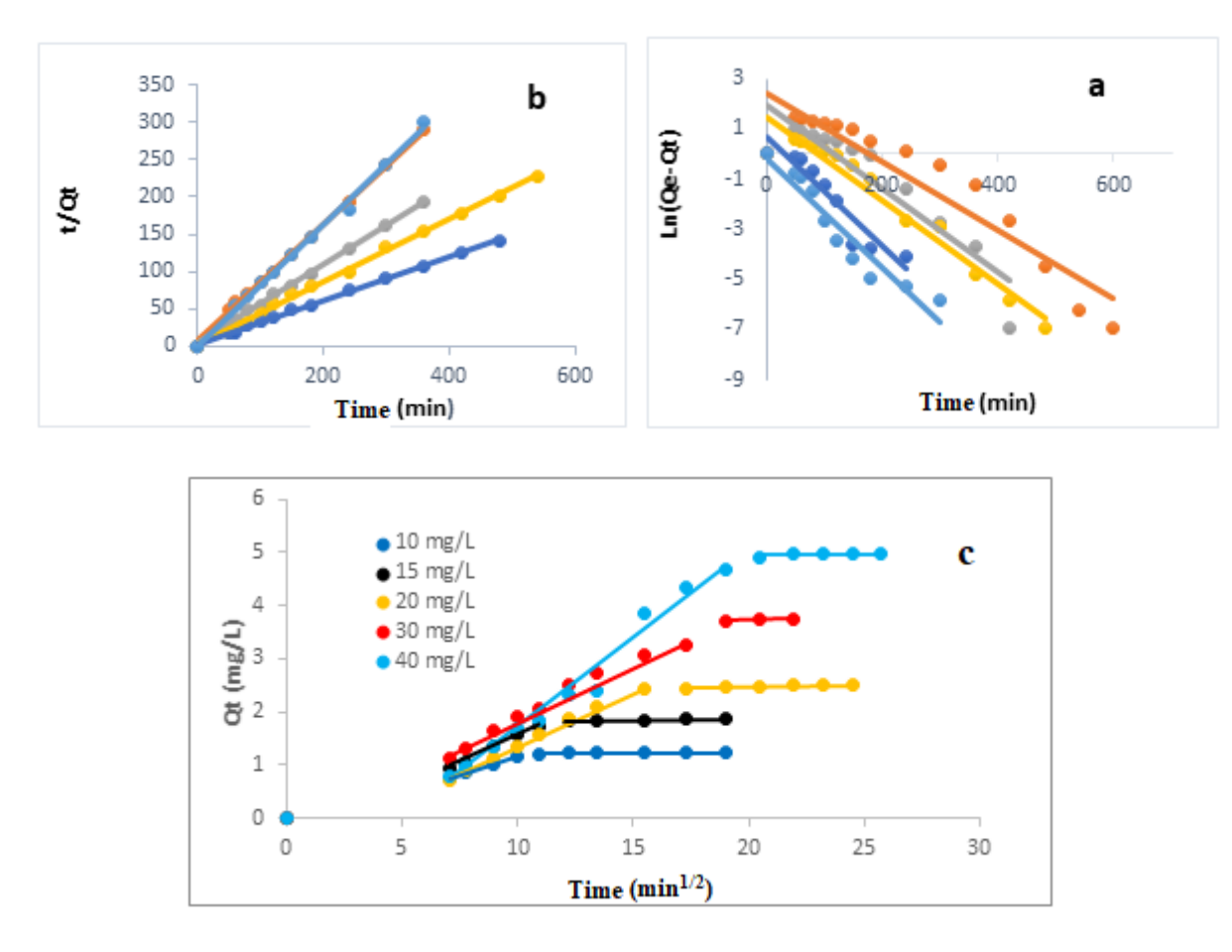


Figure 8. Kinetic models: (a): pseudo-first-order, (b): pseudo-second-order, (c): Intraparticle diffusion

> The values of the equilibrium adsorption capacity determined theoretically by the pseudo-first-order model are almost all very different from the experimental values. The coefficients of

determination are between 0.87 and 0.95 and the constants of (K_1) are all negative. This indicates that the pseudo-first-order model is absolutely not appropriate to describe the kinetics of this adsorption.

- The equilibrium adsorption capacities calculated by the pseudo-second-order model are partly closer to the experimental values. The rate constants (K_2) are positive and range from 0.03 to 0.82. The coefficients of determination (R^2) are very close to 1 $(R_2 = 0.99)$ for all initial concentrations. These results show that the pseudo-second-order model describes adsorption kinetics very well.
- From the results presented in **Figure 8c** and **Table 4** for the intraparticle diffusion model, it can be seen that the lines do not pass through the origin and the correlation coefficients are between 0.76 and 0.98. These results indicate that the diffusion of OFL into activated carbon pores is not the only step limiting adsorption kinetics (Deng *et al.*, 2015). This is confirmed by the presence of two straight lines for each concentration, thus proving the existence of two steps: the first step represents the diffusion of the outer film and through the boundary layer of the outer surface of the activated carbon. It takes place during the first few minutes of agitation, with a high adsorption rate. The second step is intraparticle diffusion characterized by a slowing of the adsorption rate. it is therefore the step limiting the adsorption rate (Deng *et al.*, 2015).

3.4 Modelling of adsorption isotherms

The adsorption isotherms of OFL on activated carbon are shown in the **Figure 9**. These linear representations obtained from the experimental values of adsorption of the OFL were used to determine the equilibrium parameters and the values of the Langmuir and Freundlich constants were calculated by linear regression (**Table 5**).

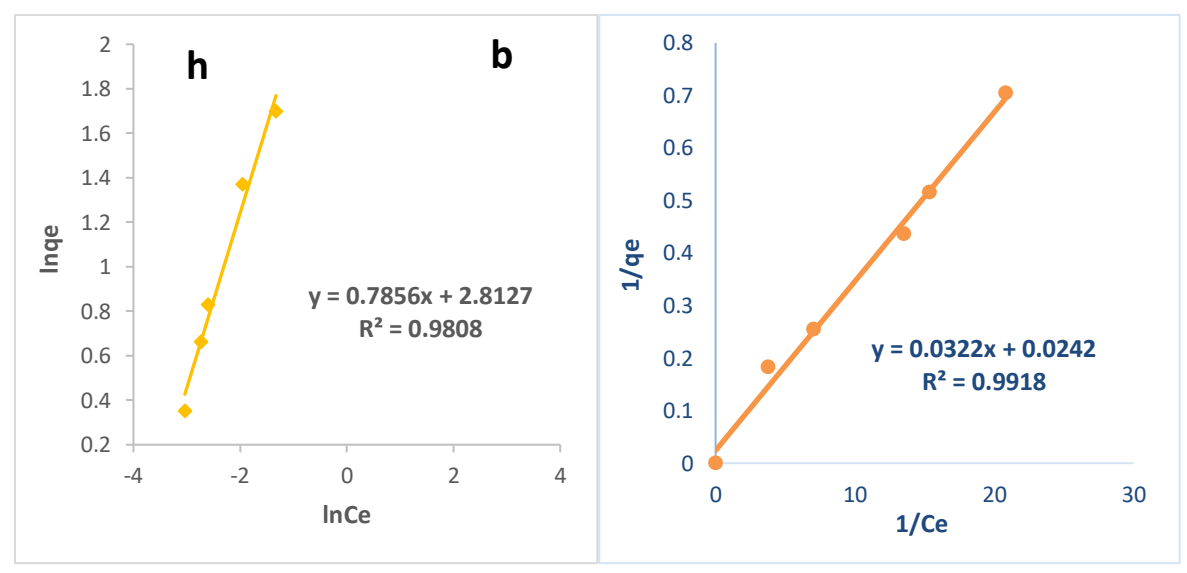


Figure 9. Modelling of the OFL adsorption isotherm on activated carbon (a): Langmuir model; (b): Freundlich model

Table 5. Parameters of OFL adsorption isotherms on activated carbon

Langmuir Isotherm			Freundlich Isotherm			
Qm (mg/g)	K _L (L/mg)	R _L	\mathbb{R}^2	$\mathbf{K}_{\mathbf{F}}$	$1/n_{\rm f}$	\mathbb{R}^2
41.32	0.75	0.03	0.99	16.65	0.78	0.98

Analysis of the results in this table reveals coefficients of determination of 0.99 and 0.98 respectively for the Langmuir and Freundlich models. Based on the values of these coefficients, the Langmuir model better describes the nature of adsorption. This suggests that the adsorption of molecules takes place on a homogeneous monolayer surface without interactions between the adsorbed molecules (Hameed *et al.*, 2007).

Conclusion

The present study showed the efficacy of activated carbon prepared from coconut shells for the removal of ofloxacin in an aqueous medium. The characterization of activated carbon revealed a microporous and mesoporous material with a high specific surface area (1195 m²/g) and an acidic character marked by pHpzc of 2.9, with a predominance of carboxylic and lactonic functions. Adsorption parameters confirmed remarkable efficacy, with percentages of ofloxacin removal of more than 99 % in 15 h. Adsorption is optimized at pH 6, with an adsorbent mass of 4 g and an initial ofloxacin concentration of 20 mg/L. Increasing the mass of the adsorbent increases the percentage of removal, while increasing the initial concentration of the adsorbate increases the adsorption capacity until the sites are saturated. The study of adsorption kinetics revealed that the pseudo-second-order model is appropriate to describe the adsorption process with a regression coefficient very high R² of 0.99. As for the adsorption isotherms, the Langmuir's model has proven to be more interesting to describe the adsorption isotherm of the experimental data. This activated carbon from coconut shells is a very effective and economical adsorbent for the removal of ofloxacin.

References

- Aaddouz M., Azzaoui K., Akartasse N., Mejdoubi E., *et al.* (2023). Removal of Methylene Blue from aqueous solution by adsorption onto hydroxyapatite nanoparticles, *Journal of Molecular Structure*, 1288, 135807, https://doi.org/10.1016/j.molstruc.2023.135807
- Abuduxike G., Aljunid S.M. (2012). Development of health biotechnology in developing countries: Can private-sector players be the prime movers? *Biotechnology Advances*, 30, Issue 6, 1589-1601, https://doi.org/10.1016/j.biotechadv.2012.05.002
- Akartasse N., Azzaoui K., Mejdoubi E., Elansari L. L., Hammouti B., Siaj M., Jodeh S., Hanbali G., Hamed R., Rhazi L. (2022), Chitosan-Hydroxyapatite Bio-Based Composite in film form: synthesis and application in Wastewater, *Polymers*, 14(20), 4265, https://doi.org/10.3390/polym14204265
- Allen A., Nilsson L. (2021). The Drug Factory: Industrializing how new drugs are found, *SLAS Discovery*, 26, Issue 9, 1076-1078, https://doi.org/10.1177/24725552211028124
- Annadurai G., Juang R.S., Lee D.J. (2002) Use of cellulose-based wastes for adsorption of dyes from aqueous solutions. *Journal of Hazardous Materials*, B92, 263–274. doi:10.1016/s0304-3894(02)00017-1
- Aydin I., Talinli (2013) Analysis occurrence and fate of commonly used pharmaceuticals and hormones in the Buyukcekmece Watershed, Turkey. *Chemosphere*, 90, 2004–2012.
- Bhatia V., Ray A.K., Dhir A. (2016) Enhanced photocatalytic degradation of ofloxacin by co-doped titanium dioxide under solar irradiation. *Sep. Purif. Technol.* 161, 1-7
- Blanco L.M.C., Martínez-Alonso A., Tascon J.M.D. (2000) Microporous Texture of activated carbon fibres prepared from nomex aramid fibres. *Micropor Mesopor Mater.*, 34, 171-179

- Calvet R., Terce M., Arvieu J.C. (1980) Adsorption des pesticides par les sols. *Ann. Agron*, 31, 239-257
- Chaturvedi P., Shukla P., Giri B., Chowdhary P., Chandra R., Pandey P. (2021) Prevalence and hazardous impact of pharmaceutical and personal care products and antibiotics in environment:

 A review on emerging contaminants. *Environmental Research*, 194.
- Chunmiao Z., Yinhai L., Ben L., Huaxuan Z. (2019) Ofloxacin Adsorption on Chitosan/Biochar Composite: Kinetics, Isotherms, and Effects of Solution Chemistry. *Polycyclic Aromatic Compounds*, 39(3), 287-297
- Dbik A., El Messaoudi N., Lacherai A. (2014). Valorisation du bois des noyaux des dattes d'une variété de palmier de la région de Tinghir (Maroc): Application à l'élimination de bleu de méthylène. *J. Mater. Environ. Sci.*, 5 (S2), 2510-2514.
- Deng L., Shi Z. (2015). Synthesis and characterization of a novel Mg-Al hydrotalciteloaded kaolin clay and its adsorption properties for phosphate in aqueous solution. *Journal of Alloys and Compounds*, 637, 188-196.
- El-Ghenymy A., Oturan N., Oturan M., Garrido J., Cabot P.L., Centellas F., Rodríguez R. (2013) Comparative electro-Fenton and UVA photoelectro-Fenton degradation of the antibiotic sulfanilamide using a stirred BDD/air-diffusion tank reactor. *Chem. Eng. J.*, 234:115–123.
- Foo K.Y., Hameed B.H. (2012) Coconut husk derived activated carbon via microwave induced activation: Effects of activation agents, preparation parameters and adsorption performance. *Chemical Engineering Journal*, 184, 57–65
- Hameed B. H. (2010) Evaluation of papaya seed as a novel non-conventional low-cost adsorbent for removal of methylene blue. *J. Hazard. Mater*, 162:939–994.
- Hameed B. H., Ahmad A. L., Latiff K. N. A. (2007) Adsorption de colorant basique (bleu de méthylène) sur charbon actif préparé à partir de sciure de rotin. *Dyes and Pigments*, 75:143–149.
- Hapeshi E., Achilleos A., Vasquez M., Michael C., Xekoukoulotakis N., Mantzavinos D., Fatta-Kassinos D. (2010) Drugs degrading photo- catalytically: kinetics and mechanisms of ofloxacin and atenolol removal on titania suspensions. *Water Res*.
- Hassan S.A., Ali F.J. (2014) Assessement of the Ofloxacin (Novecin) Adsorption from aqueous solutions by Two Agricultural Wastes. *International Journal of Advanced Scientific and Technical Research*, 2(4), 950-965
- Hidayu A.R., Muda N. (2016) Preparation and characterization of impregnated activated carbon from palm kernel shell and coconut shell for CO2 capture. *Procedia Engineering*, 148, 106 113
- Ho Y.S., McKay G. (1999) A Multi-stage Batch Sorption Design with Experimental Data. *Adsorpt. Sci. Technol.*, 17, 4, 233-243. https://doi.org/10.1177/026361749901700401
- Inbaraj B.S., Sulochana N. (2006) Mercury adsorption on a carbon sorbent derived from fruit shell of Terminalia catappa. *J. Hazard. Mater*, 133, 283–290.
- Klein E., Van Boeckel T., Martinez M., Pant S., Gandra S., Levin S., Goossens A., Laxminarayan H. (2018) Global increase and geographic convergence in antibiotic consumption between 2000 and 2015. *Proceedings of the National Academy of Sciences*, 115(15).
- Kumar V.S.H., Huligowda L.K.D, Umesh M., Chakraborty P., *et al.* (2025). Environmental Pollutants as Emerging Concerns for Cardiac Diseases: A Review on Their Impacts on Cardiac Health. *Biomedicines.* 13(1), 241. https://doi.org/10.3390/biomedicines13010241
- Lagergren S., Svenska B.K. (1898) Zur theorie der sogenannten adsorption geloester stoffe (About

- the theory of the so called adsorption of solved substances), *Vetenskapsakad. Handl*, 24, 1–39 Lahouidak S., Soriano M.L., Salghi R., Zougagh M., Ríos Á.J.E. (2019) Graphene quantum dots for
- Lahouidak S., Soriano M.L., Salghi R., Zougagh M., Ríos A.J.E. (2019) Graphene quantum dots for enhancement of fluorimetric detection coupled to capillary electrophoresis for detection of ofloxacin, *Electrophoresis*, 40, 2336-2341ac
- Lubna A., Mahtab A., Sajid I., Ahmed A., Abdelhafez M.T.M. (2021) Biochars' adsorption
- performance towards moxifloxacin and ofloxacin in aqueous solution: Role of pyrolysis temperature and biomass type. *Environmental Technology & Innovation*, 24, 101912. https://doi.org/10.1016/j.eti.2021.
- Madehi N., Tay K. (2015) Ozonation of ofloxacin in water: byproducts, degradation pathway and ecotoxicity assessment. *Sci Total Environ*, 520:23–31.
- Maheshwari M., Vyas R.K., Sharma M. (2013) Kinetics, equilibrium and thermodynamics of
- ciprofloxacin hydrochloride removal by adsorption on coal fly ash and activated alumina. *Desalinat. Water Treat.*, 51(37-39), 7241-7254.
- Nguyen V., Nguyen H., Vranova V., Nguyen L., Khieu Q. (2021). Artificial neutral network modeling for Congo red adsorption on microwave-synthesized akageneite nanoparticles, optimization, kinetics, mechanism, and thermodynamics. *Environ. Sci. Pollut. Res. Int.*, 28:9133–9145.
- Pandey P., Sharma S., Sambi S. (2010). Kinetics and equilibrium study of chromium adsorption on zeoliteNaX .*Int. J. Environ. Sci. Tech.*, 7 (2), 395–404.
- Patil A., Shrivastava V. (2010). Alternanthera bettzichiana plant powder as low cost adsorbent for removel of congo red from aqueous solution. *Int. J. Chemtech Res.* 2, 842–850.
- Rivera-Utrilla M., Sanchez-Polo A., Ferro-Garcia G., Prados-Joya R., Ocampo-Perez. (2013) Pharmaceuticals as emerging contaminants and their removal from water. *A review, Chemosphere*, 93, 1268–1287.
- Salem B. S., Mezni M., Errami M., Amine K.M., Salghi R., Ali. Ismat H., Chakir A., Hammouti B., Messali M., Fattouch S. (2015), Degradation of Enrofloxacin Antibiotic under Combined Ionizing Radiation and Biological Removal Technologies, *Int. J. Electrochem. Sci.*, 10 N°4, 3613-3622, https://doi.org/10.1016/S1452-3981(23)06565-3
- Sbardella L., Comas J., A. Fenu J., Rodriguez-Roda I., Weemaes M. (2018) Filtre à charbon actif biologique avancé pour supprimer les produits pharmaceutiques composés chimiquement actifs provenant des eaux traitées. *Sci. Total Environ*, 636, 519–529.
- Sogbochi E., (2023) Elaboration par voies thermochimiques de charbons actifs dérivés de coproduits de Lophira lanceolata : essais d'adsorption de micropolluants de l'eau. *Université d'Abomey-Calavi*, P 176.
- Tan I.A., Ahmad A.L., Hameed B.H. (2009) Adsorption isotherms, kinetics, thermodynamics and desorption studies of 2, 4, 6-trichlorophenol on oil palm empty fruit bunch-based activated carbon. *J. Hazard. Mater*, 164, 473–482. http://dx.doi.org/10.1016/j.jhazmat.2008.08.025
- Thomas T. (2015) L'adsorption des produits pharmaceutiques par interactions organominerales : processus et applications environnementales. Sciences de la Terre. *Université d'Orleans, France*.
- Tra B. T. D., Soro Y., Briton B.G.H. (2024) Optimization of the conditions for preparation of Activated Carbons from Blighia sapida (Sapindaceae) shells, *J. Mater. Environ. Sci.*, 15(12), 1825-1837
- Vunain E., Kenneth D., Biswick T. (2017) Synthesis and characterization of low-cost activated carbon prepared from Malawian baobab fruit shells by H3PO4 activation for removal of Cu(II) ions: equilibrium and kinetics studies. *Applied Water Science*, 7, 4301-4319.

- Wang H., Xi H., Xu L., Jin M., Zhao W., Liu H. (2021) Effets écotoxicologiques, devenir environnemental et risques des produits pharmaceutiques et de soins personnels dans l'environnement aquatique. *Sci. Environ*, 788.
- Wang W., Lemaire R., Bensakhria A., Luart D. (2022) Review on the catalytic effects of alkali and alkaline earth metals including sodium, potassium, calcium and magnesium on the pyrolysis of lignocellulosic biomass and on the co-pyrolysis of coal with biomass. *J. Anal. Appl. Pyrolysis*, 163.
- Weber T.W., Chakravo R.K. (1974) Pore and Solid Diffusion Models for Fixed-Bed Adsorbers. *AIChE Journal*, 20, 228-238. http://dx.doi.org/10.1002/aic.690200204
- Yakou S.M., Sharaf El-Deen G. (2016) Characterization of activated carbon prepared by phosphoric acid activation of olives stones. *Arabian Journal of Chemistry*, 9, 1155-1162
- Zabihi M., Haghighi ASL A., Ahmadpour A. (2010). Studies on adsorption of mercury from aqueous solution on activated carbons prepared from walnut shell. *J. Hazard. Mater*, 174, 251–256

(2025); http://www.jmaterenvironsci.com